CHEMISTRY
A EUROPEAN JOURNAL

DOI: 10.1002/chem.200800746

Supramolecular Synthons on Surfaces: Controlling Dimensionality and Periodicity of Tetraarylporphyrin Assemblies by the Interplay of Cyano and Alkoxy Substituents

Nikolai Wintjes,*[a] Jens Hornung,*[b] Jorge Lobo-Checa,[a] Tobias Voigt,[b] Tomáš Samuely,[a] Carlo Thilgen,[b] Meike Stöhr,[a] François Diederich,*[b] and Thomas A. Jung*[c]

Abstract: The self-assembly of three porphyrin derivatives was studied in detail on a Cu(111) substrate by means of scanning tunneling microscopy (STM). All derivatives have two 4-cyanophenyl substituents in diagonally opposed *meso*-positions of the porphyrin core, but differ in the nature of the other two *meso*-alkoxyphenyl substituents. At coverages below 0.8 monolayers, two derivatives form molecular chains, which evolve into nanoporous networks at higher coverages. The third derivative self-assembles directly into a nanoporous network without showing a one-dimensional phase. The pore-to-pore distances for the three networks depend on the size and shape of the alkoxy substituents. All observed effects are explained by 1) different steric demands of the alkoxy residues, 2) apolar (mainly dispersion) interactions between the alkoxy chains, 3) polar bonding involving both cyanophenyl and alkoxyphenyl substituents, and 4) the entropy/enthalpy balance of the network formation.

Keywords: molecular recognition · networks on surfaces · porphyrinoids · scanning probe microscopy · supramolecular chemistry

Introduction

Complex molecular layers on surfaces with engineered architectures and properties[1] are expected to play an important role in the development of future devices at the nanoscale.[2] In contrast with the three-dimensional crystal packing of molecules or tectons, which has been the focus of research for many years,[3] surface and interface self-assemblies allow the addressing of individual units.[4,5] To control the self-assembly process on the surface,[6] a detailed understanding of the molecule–surface and intermolecular interactions involved is crucial. Their interplay can lead to a variety of phases for the same coverage,[7,8] but the observed phases can also depend on the surface coverage.[9] In the latter case, several phases might coexist for a small coverage region,[10] or a transition from one phase to the other occurs.[11]

Since the invention of STM in 1981, a significant number of two-dimensional patterns at the solid–liquid and the solid–vacuum interface has been reported.[12] Among them, there are some striking examples of self-assemblies that are guided, for example, by solvent interactions,[13] surface prepatterning,[14] molecular symmetry,[15] the use of elaborated binding motifs as they are found in hydrogen bonding,[16] interactions among polar groups,[17] metal complexation,[18] or by exploiting the interactions of long alkyl chains with the underlying substrate, especially on highly ordered pyrolytic graphite (HOPG).[19]

Particularly interesting self-assemblies, in view of future applications, are 1) molecular chains because of their potential to act as organic wires and 2) porous networks due to their capability to recognize[20,21] and host molecular

[a] Dr. N. Wintjes, Dr. J. Lobo-Checa, T. Samuely, Dr. M. Stöhr
Department of Physics, University of Basel
4056 Basel (Switzerland)
Fax: (+41) 61-267-3784
E-mail: n.wintjes@unibas.ch

[b] J. Hornung, Dr. T. Voigt, Dr. C. Thilgen, Prof. Dr. F. Diederich
Laboratorium für Organische Chemie, ETH-Zürich
Hönggerberg, HCI, 8093 Zürich (Switzerland)
Fax: (+41) 44-632-1109
E-mail: hornung@org.chem.ethz.ch
diederich@org.chem.ethz.ch

[c] Dr. T. A. Jung
Laboratory for Micro- and Nanotechnology
Paul Scherrer Institute, 5232 Villigen PSI (Switzerland)
Fax: (+41) 56-310-2646
E-mail: thomas.jung@psi.ch

Supporting information for this article is available on the WWW under http://www.chemeurj.org/ or from the author.

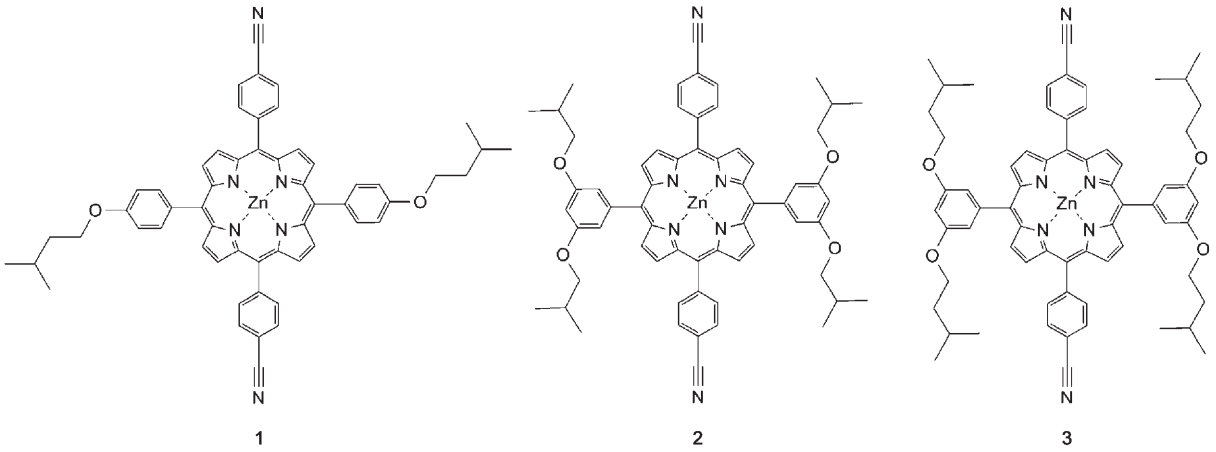

Scheme 1. Chemical structures of the three porphyrin derivatives **1**–**3** used in this study.

guests.[5,17,22] Previous work has shown that it is possible to modify the pore dimensions of such networks by changing the entire structure of the molecular building block.[8,23] So far, however, no systematic study has focused on how the variation of functional subunits attached to the same molecular core influences the structures of self-assembled porous layers on metal surfaces.

Molecules **1**–**3** (Scheme 1) investigated in the present study are derived from the well-established tetrakis(*meso*-phenyl)porphyrin core.[24,25] Their *meso*-(4-cyanophenyl) groups were expected to undergo dipolar[26] and C–H···N≡C hydrogen-bonding interactions,[22] thereby providing the main ordering and orienting ingredient for network formation on surfaces. Such structural motifs, assembled by intermolecular interactions between functional groups, have been defined by Desiraju as "supramolecular synthons" and used for the planning of supramolecular assemblies.[27,28] Supramolecular synthons composed of two or three 4-cyanophenyl groups had initially been observed in 3D crystals,[29] and their linear dimeric and cyclic trimeric interaction motifs (**A** and **B** in Scheme 2) have been found to enforce the formation of distinct crystal lattices. Similar structural motifs have also recently been introduced to form defined supramolecular assemblies on surfaces.[4,17,20,22,30] As a novel feature, variable functional alkoxy subunits were introduced in this work to further control the nature of the desired assemblies. The two (in **1**) or four alkoxy groups (in **2** and **3**) have different spatial demands and undergo not only apolar (mainly dispersion) interactions with each other, but can also participate in polar interactions that stabilize the networks. Another important feature of the alkoxy residues is their tendency to "condense" or exhibit fluidlike dynamic behavior depending on the environmental conditions,[31] as is well known from liquid crystals.[32]

Herein, we present a systematic study on the influence of the different alkoxyphenyl substituents in porphyrins **1**–**3** on the resulting supramolecular arrangements at the solid–vacuum interface by using the concept of synthons for supramolecular surface assemblies.[28] The architecture as well as the temperature-activated mobility and corresponding steric requirement of the alkoxyphenyl residues are identified as the key parameters governing the resulting structures, that is, one-dimensional molecular chains or two-dimensional porous layers. Furthermore, we provide evidence that advanced structural control is not only ensured by the well-known supramolecular synthons **A** and **B** shown in Scheme 2, but also that spatial requirements and apolar as well as polar interactions of the alkoxyphenyl substituents induce additional assembly modes (**C** and **D** in Scheme 2).

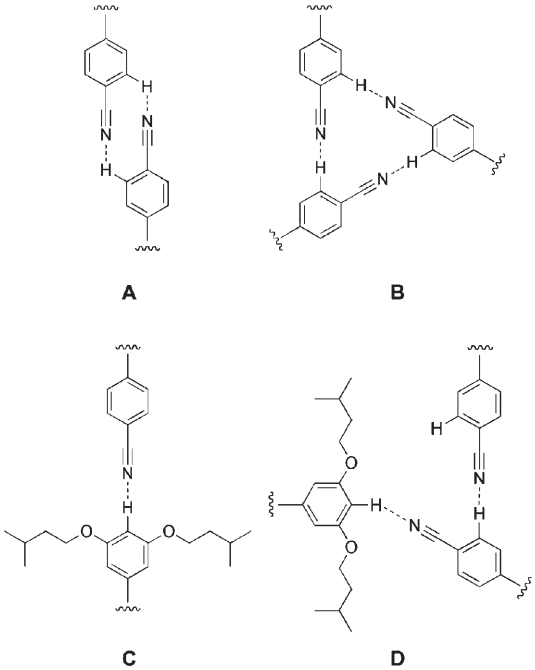

Scheme 2. Examples of supramolecular synthons formed by two (**A**) or three (**B**) interacting 4-cyanophenyl groups, as well as those formed by the interaction of the 4-cyanophenyl group with a 3,5-alkoxyphenyl group (**C** and **D**).

Results and Discussion

Appearance of the molecular compounds in STM images: The selected molecular building blocks **1**–**3** (Scheme 1) were sublimed onto a Cu(111) substrate at sub-monolayer coverages. Consistent with earlier observations,[33] the influence of the STM tip leads, for all three derivatives, mainly to two different imaging modes in which either the π system provides the dominant contrast ("π-imaging mode", Figure 1a and c), or all parts of the molecule are equally visible ("full imaging mode", Figure 1b and d). In the π-imaging mode, the porphyrin ring is imaged as two opposing lobes separated by a dark line. This appearance is caused by a saddle-shaped deformation of the porphyrin ring induced by steric hindrance between the pyrrolic hydrogen atoms (β-hydrogen atoms) of the core and hydrogen atoms of the *meso*-phenyl rings.[34] Consequently, two pyrrole rings are tilted upwards and provide strong contrast in the STM images, whereas the other two rings are tilted downwards and appear as a dark line (Figure 1a). The four phenyl rings can be recognized as four lobes in close vicinity to the porphyrin ring, each providing nearly the same contrast as the pyrrole rings that are tilted upwards. These features allow for a precise identification of an individual molecule even inside a network (see the superimposed molecular structure in Figure 1a). The mode of imaging (π- or full imaging mode) is not influenced by the applied voltage. However, by using voltage pulses of around 3.5 V and 50 ms, one can randomly switch between imaging modes (see the Supporting Information). Hence, it is plausible that the different modes are caused by subtle changes of the tip, for example, caused by an adsorbate on the tip apex, as also observed in other STM studies.[35]

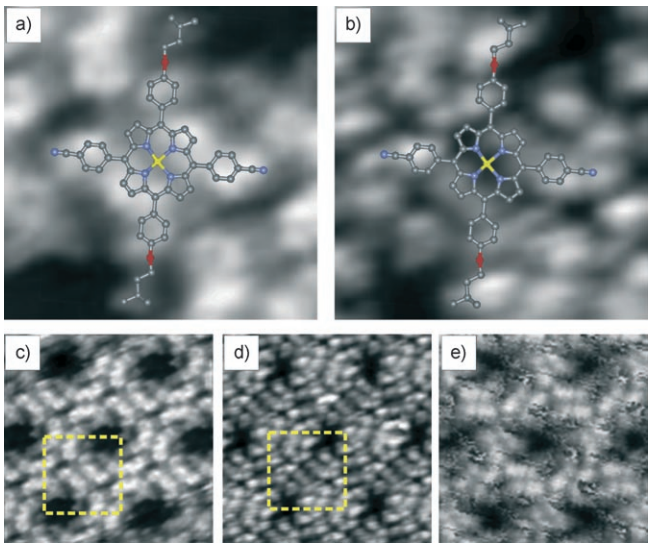

Figure 1. STM images showing different appearances of porphyrin derivative **1** on Cu(111) at coverages >0.8 ML (ML = monolayer). a) and b) represent the parts of c) and d), respectively, that are enclosed by the dashed rectangles. They show an individual molecule inside the network of **1**. Two different imaging modes could be observed depending on the tip conditions: in a) and c) the π system of the molecules is pronounced (c: 7.5×7.5 nm^2, $U=-0.8$ V, $I=16$ pA), in b) and d) all parts of the molecules provide equal contrast (d: 7.5×7.5 nm^2, $U=-1.3$ V, $I=24$ pA). e) An image of derivative **2** showing that mobile parts of the molecules can lead to characteristic "streaks" in STM images (7.5×7.5 nm^2, $U=-2.5$ V, $I=20$ pA).[36]

Depending on the scanning conditions, sections of the STM images may show a characteristic fuzzy signal regardless of the imaging mode (Figure 1e[36]). These streaks can be related to parts of the molecules that move while being passed by the scanning tip.[37] For the present systems, we attribute this effect to the mobility of the alkoxy chains. The streaks diminish with increasing proximity of tip and sample. This can be associated with an increasing interaction between the scanning tip and the alkoxy chains, which are thereby pushed aside.[38]

Self-assembly at coverages <0.8 monolayer: For porphyrin **1**, we observed self-assembly into a nanoporous, hexagonal network with *p*3 symmetry even at coverages <0.05 ML (ML = monolayer; Figure 4a, left), after the well-known initial decoration of the step edges.[39] This network exhibits the same internal geometry as previously published porphyrin assemblies[22] and will be described in more detail in the section on tailored nanoporous networks. In contrast, molecules **2** and **3** form long chains with the same characteristics for both derivatives after decorating the step edges and for molecular coverages up to approximately 0.8 ML (Figure 2a). The chains nucleate either at one of the molecules decorating the step edges or at a defect on a terrace and are stable up to at least 200 K. At room temperature, the molecules are observed in a 2D mobile phase.[40]

Within the chains of **2** and **3**, single molecules can be clearly identified (Figure 2b, top). The porphyrin core and the phenyl rings appear as described above for the π-imaging mode. The cyano groups are not resolved. The alkoxy chains appear as one lobe each, situated above and below the porphyrin ring and the 4-cyanophenyl substituents. No significant difference in the appearance of molecules **2** and **3** was found in the STM images.

A closer analysis reveals that the chains exhibit mainly two interconnecting modes for adjacent molecules. The first one is a "straight" connection which simply elongates the chain (circle a in Figure 2a). The second one leads to a "kink" (circle b), which changes the direction of the chain, mostly by approximately 30 degrees. Also, sections are found in which a kink towards one side is immediately followed by a kink towards the other side, leading to a zigzag type, overall straight section (circle c).

Most probably, in a straight connection the cyano groups, which are not visible in the STM images, are lying antiparallel and interact through dipole–dipole interactions, and benefit additionally from C−H···N≡C interactions, as shown for molecules 3 and 4 in Figure 2b, bottom.[41] This type of interaction corresponds to the dimeric supramolecular synthon **A** in Scheme 2 and was theoretically described by Y. Okuno et al. for a benzonitrile dimer on a Au(111) surface[42] and is also known in the gas phase[43] and in organic crystals.[44]

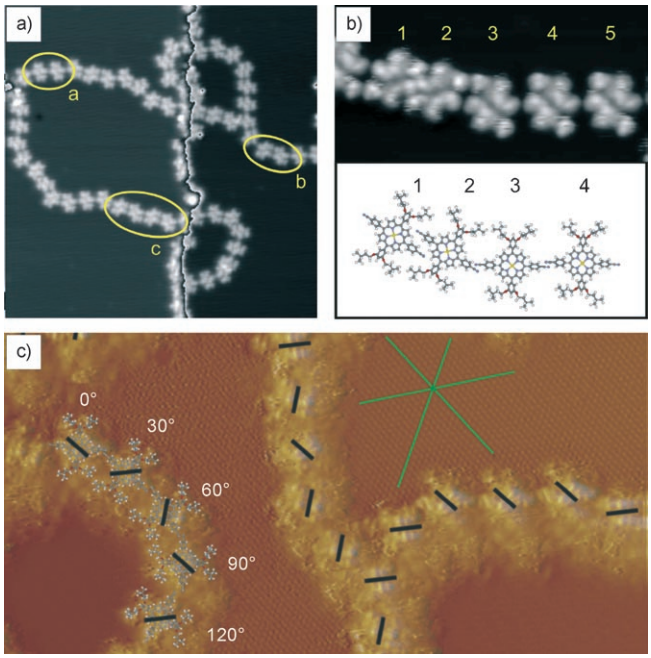

Figure 2. STM images showing the arrangements of porphyrins **2** (a and b) and **3** (c) on Cu(111) at coverages <0.8 ML (see also the Supporting Information). Both molecules arrange in chainlike structures and individual molecules can be clearly identified. a) STM image showing typical chains formed by molecule **2** (41×41 nm^2; $U=-1.5$ V, $I=20$ pA. The color scale of the image was adjusted to provide good contrast at the terraces for highlighting the molecular features. A step edge, seen in the image as a black line, runs vertically from top to bottom.). b) Top: A detailed STM image (12×6 nm^2; $U=-1.6$ V, $I=11$ pA) showing the main types of connections between adjacent molecules in the molecular chains. Bottom: A tentative model, generated with Spartan,[41] for the intermolecular interactions within the chains. c) Simultaneous imaging (12.5×25 nm^2; $U=+0.9$ V, $I=10$ pA) of molecular chains of **3** and substrate atoms of Cu(111). The orientation of the characteristic dark lines (see description in the main text) is marked by black lines, which allow for an easy correlation with the principal directions of the substrate (green star).

Sometimes, a small variation of this bonding motif can be found, as seen for molecules 1 and 2 in Figure 2b, bottom. Here, the molecules in a straight section are lying closer together and show a small vertical and lateral displacement. Our calculations indicate that this arrangement benefits from a weak C≡N···H–C hydrogen bond between the cyano group and the β-hydrogen atoms of the porphyrin ring, as indicated by the molecular model in the lower part of Figure 2b.[41] Within the kinks, the dipole–dipole interaction is weakened because the dipoles are not perfectly antiparallel in such an arrangement (molecules 2 and 3 in Figure 2b, bottom). Nevertheless, this loss in interaction energy may be partially compensated by van der Waals interactions of the alkoxy chains,[45] which are closer together than in the straight sections.

Influence of the underlying Cu(111) surface on the porphyrin chain formation: In solution, a temperature dependent, hindered rotation around the single bond connecting the *meso*-aryl substituents to the porphyrin core is observed.[46] After adsorption on the metal surface, however, the dihedral angle between the *meso*-aryl and porphyrin planes is typically fixed in a position that depends on the interaction with the substrate.[25] Consequently, two conformational isomers corresponding to a positive or negative tilt angle of the alkoxyphenyl substituents are observed upon adsorption. In STM images, these can be distinguished by the relative orientation ($+45$ or $-45°$) of the characteristic diagonal dark line with regard to the cyanophenyl substituents (cf. molecules 2 and 3 in Figure 2b, top). The two conformational isomers are found with equal probabilities for all three porphyrins studied herein, which is in agreement with earlier observations.[47] Conformers exhibiting parallel rotation around opposite aryl–porphyrin bonds have not been identified in our study. By analyzing STM images that exhibit both good resolution of the adsorbed molecules and atomic resolution of the substrate (Figure 2c), it becomes apparent that the characteristic dark lines are also aligned with the main atomic directions of the supporting substrate (green star in Figure 2c) within an accuracy of $\pm5°$. This observation, in combination with the two possible orientations of the dark line with respect to the axis through the two cyanophenyl rings, can explain the changes in direction of 30° within a kink: Two different enantiomers, which are adjacent within a chain (as molecules 2 and 3 in Figure 2b, top) and are aligned along different principal directions of the threefold symmetric (111) substrate, exhibit a relative orientation of $(120-(2\times45))°=30°$. In contrast, adjacent but identical enantiomers (as molecules 3 and 4 in Figure 2b, top), which are aligned along the same principal directions, form a straight connection. In the STM images, this is revealed by the observation that in a straight connection two adjacent molecules look like perfect copies of each other (with the orientation of the dark lines), whereas in a kink they appear as mirror images. Notably, this result shows that within the chains an intermixing of the two different conformational enantiomers occurs. For two-dimensional assemblies of similar porphyrin derivatives, long-range interactions that extend beyond nearest neighbors have also been reported.[20] However, no clear evidence for such interactions was found here, since they should lead to a preferred arrangement with either straight, curved, or zigzagged chain sections.

Branching of the porphyrin chains: Next to the two types of intermolecular connection modes observed in linear chain sections, three different types of branching arrangements were observed (Figure 3). For the first one (Figure 3a), a cyano group of one molecule undergoes favorable C≡N···H–C hydrogen bonding with a β-hydrogen atom of the porphyrin core or a hydrogen atom in the *meta* position to the nitrile group in a 4-cyanophenyl ring of an adjacent molecule. This motif has been found for both molecules **2** and **3**. In a second dimeric branching arrangement (Figure 3b), the 4-cyanophenyl group of one molecule forms a C≡N···H–C hydrogen bond with the C–H group *ortho* to the two alkoxy substituents of one phenyl ring of a second

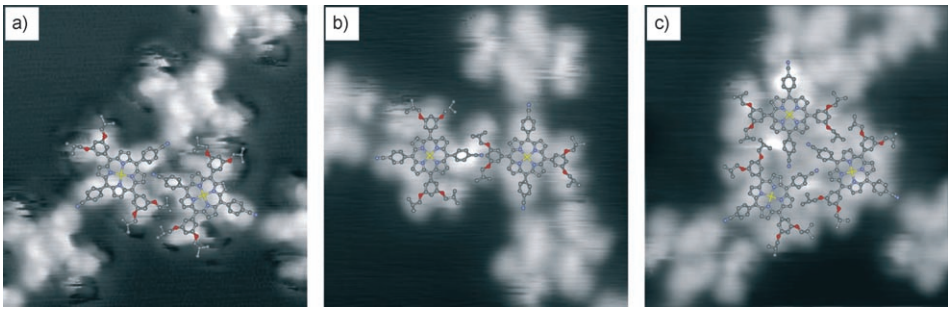

Figure 3. High-resolution STM images (6.4×6.4 nm^2; $U=-1.5$ V, $I=20$ pA) of molecule **2** on Cu(111) showing three different types of branching points for the molecular chains. Types a) and b) can be also found for molecule **3**. a) Branching by C≡N···H–C hydrogen-bond formation between the cyano group of one molecule and C–H groups on the porphyrin core and/or the 4-cyanophenyl substituent of another molecule. b) Branching by a C≡N···H–C hydrogen bond between the cyano group of one molecule and the C–H residue *ortho* to the alkoxy substituents on the phenyl ring of another molecule. c) Branching induced by a trimeric cyanophenyl array, such as that shown for the trimeric synthon **B** in Scheme 2.

molecule (cf. **C** in Scheme 2). This hydrogen bond benefits from the substantial polarization of the C–H$^{\delta+}$ residue *ortho* to two electronegative oxygen atoms. Secondary repulsive N···O interactions[48] are minimized because the lone pairs of the sp^2-hybridized oxygen atoms point away from the negatively polarized nitrogen atom of the C≡N group. This type of dimeric branching, which is again observed for both molecules **2** and **3**, clearly demonstrates that the introduction of the alkoxy substituents enables new self-assembling motifs, which could also be viewed as new supramolecular synthons. A dimeric structure similar to **C** has already been reported in crystal structures,[49] but is so far unknown on the surface. The formation of a third association motif (Figure 3c), a cyclic trimeric arrangement of cyanophenyl moieties resembling the trimeric supramolecular synthon **B** in Scheme 2, was observed exclusively for molecule **2**. Within this trimeric assembly, a cyanophenyl group of each molecule acts as hydrogen-bond acceptor (C≡N) towards one and as a donor (C–H) towards the other partner, thereby interconnecting three molecules with three hydrogen bonds. Similar trimeric arrangements have been reported in the literature for cyanophenyl derivatives in the gas phase,[43] in two-dimensional assemblies,[22,30,42] and also in 3D crystal structures.[50]

Self-assembly at coverages >0.8 monolayer: Tailored nanoporous networks: Above a coverage of approximately 0.8 ML, all three porphyrins **1**–**3** self-assemble into nanoporous, hexagonal networks with *p*3 symmetry (Figure 4). We were able to develop a tentative model for each of the three networks, guided by the following aspects: First, we compared the networks observed in the present study to a network previously reported by our group, which is formed by a similar porphyrin derivative.[22] Second, we took advantage of the π-imaging mode, which allowed reliable identification of single molecules inside the network. Finally, we related the fuzzy parts observed in some STM images (see above) with the alkoxy chains.

The nanoporous network formed by compound **1**, which can be observed at all submonolayer coverages >0.05 ML (we will refer to it as network 1; Figure 4a, left), exhibits a pore-to-pore distance of (30.9±2.0) Å. The unit cell contains one pore and three molecules. The model (Figure 4a, right) reveals that the pores are chiral. Thus, in contrast with the case of the chains formed by **2** and **3**, in which an intermixing of the two conformational enantiomers was observed, for nanoporous network 1 a separation of the two conformational enantiomers occurs and consequently two types of enantiomerically pure domains can be found on the copper surface.[51] The pores are formed by the alkoxy chains of six different molecules, each of which is part of two neighboring pores. Through this, network 1 benefits from dispersion interactions from the six alkoxy groups converging into each pore. The network is furthermore stabilized by a so far unknown trimeric supramolecular synthon: the 4-cyanophenyl groups and β-hydrogen atoms of three adjacent porphyrins form a cyclic arrangement with three C≡N···H–C hydrogen bonds (blue circle in Figure 4a). In network 1 the alkoxyphenyl and cyanophenyl groups are spatially separated from each other: the former reside in the pores, whereas the latter are found inside the network.

Molecule **2** forms a network (network 2; Figure 4b, left) with a pore-to-pore distance of (33.5±1.2) Å, which is slightly larger (about 8%) than that of network 1. Again, the unit cell contains one pore and three molecules per unit cell. According to the model (Figure 4b, right), the structures of network 2 and network 1 are similar: The pores are chiral and surrounded by six molecules, in which each molecule is shared by two pores. The alkoxy groups converge into the pores, whereas the three cyanophenyl groups are involved in a trimeric interaction motif. However, this time the porphyrin core does not participate in the trimers, but instead hydrogen bonding involves C≡N and H–C moieties from 4-cyanophenyl substituents of three adjacent porphyrins (blue circle in Figure 4b). This interaction type is the same as that found for the branching mechanism shown in Figure 3c and resembles the trimeric supramolecular synthon **B** in Scheme 2. The space required for this motif is slightly higher than that for the similar trimeric arrangement in network 1 (cf. the blue circles in Figure 4a and b), which explains why the pore-to-pore distance in network 2 is slightly larger than that in network 1.

Molecule **3**, which differs from molecule **2** only by the increased length of the alkoxy chains, forms a network (network 3; Figure 4c, left) with a pore-to-pore distance of (48.0±1.4) Å, which is significantly larger than the distances

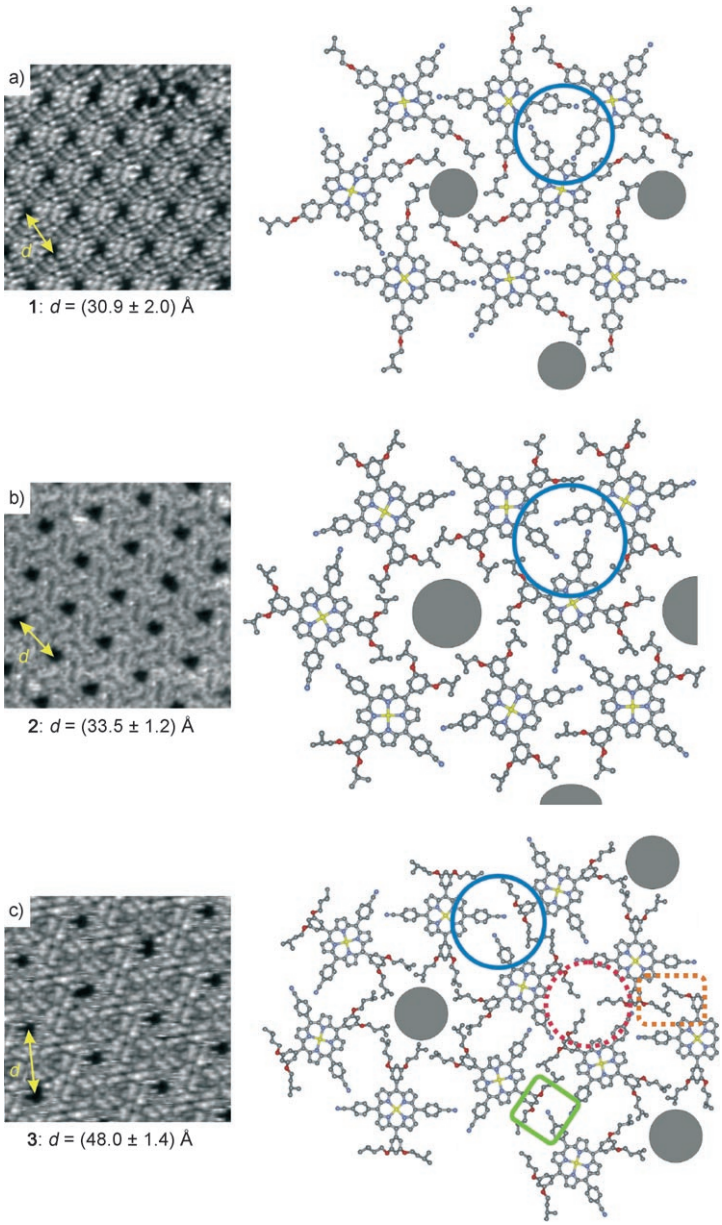

Figure 4. Left: STM images (all 15×15 nm^2; a) $U=-1.3$ V, $I=24$ pA; b) $U=-1.5$ V, $I=20$ pA; c) $U=-0.4$ V, $I=17$ pA) of the nanoporous networks (network 1 (a), network 2 (b), and network 3 (c)) formed by porphyrins **1**–**3** at coverages close to one monolayer. The networks exhibit different pore-to-pore distances *d*. Right: Tentative models of the three networks. The filled gray circles indicate the positions of the pores. The colored circles and rectangles indicate different bonding arrangements stabilizing the network (see text for details). The pores in c) exhibit characteristic streaks that indicate the mobility of the alkoxy chains.

in network 1 and network 2 (by about 43 and 55%, respectively). Remarkably, in this network the unit cell still contains one pore, whereas the number of molecules enclosed is doubled to six molecules. As a common characteristic, a single pore is formed by six molecules (Figure 4c, right). But unlike in the other two networks, each molecule belongs distinctly to one pore, which leads to the significantly larger pore-to-pore distance. The mechanism for self-assembly is truly remarkable, which shows the interplay of alkoxyphenyl and cyanophenyl rings. An asymmetric trimeric motif (blue circle in Figure 4c, cf. **D** in Scheme 2) forms in which one cyanophenyl substituent acts both as a hydrogen-bond donor and as an acceptor. It forms a C–H···N≡C hydrogen bond with the cyanophenyl substituent of a second molecule of **3** and, additionally, interacts through its C≡N group with the positively polarized hydrogen of the C–H moiety *ortho* to the two alkoxy substituents in the phenyl ring of a third molecule of **3** (see also green rectangle in Figure 4c). The latter interaction had already been observed in the branching mechanism shown in Figure 3b. A trimeric structure similar to **D** has not yet been reported. Additional stabilizing interaction motifs become apparent in network 3, caused by the imperfect separation of the two synthons used: Two (orange rectangle) or three (red circle) alkoxy chains, which are found outside the pores, interact through van der Waals dispersion forces, thereby further stabilizing the network. The hereby formed "apolar pockets" (red circle) can hardly be seen in the STM images.

Thermodynamic considerations for the formation of the chains and networks: Self-assembled structures are formed by reversible association of molecular building blocks, thereby representing thermodynamic minima.[52] To explain the phenomena described in this manuscript, one has to take into account the different energy contributions guiding the formation of networks and chains on the surface. First of all, depending on the strength of the molecule–surface and intermolecular interactions, organic adsorbates on surfaces tend to maximize the coverage (molecules per area) and even a rearrangement into a new phase can be preferred over a second layer arrangement.[40,53] Next, due to the considerably weaker intermolecular interaction energies in the supramolecular aggregates, when compared with covalent bonding, the interplay of entropy and enthalpy is of much higher importance here.[52] Finally, on threefold symmetric surfaces, the 4-cyanophenyl group is known to favor a dimeric arrangement with antiparallel dipoles or a cyclic trimer (**A** and **B** in Scheme 2).[30,42] In this work, we additionally discovered two supramolecular synthons, which involve interactions between both cyanophenyl and alkoxyphenyl substituents (**C** and **D** in Scheme 2). Due to the complexity of the presented surface assemblies, accurate numerical calculations are not straightforward. However, the observed structures have to correspond to an energetically optimized interplay of the aforementioned contributions.

Network 1 (Figure 4a) features different remarkable characteristics: although it is a porous phase, the fraction of covered surface area, as determined from STM images, is >90%. A segregation of the less polar alkoxyphenyl substituents from the more polar cyanophenyl moieties is observed. The alkoxy chains interact with each other in the pores through van der Waals forces, whereas outside the pores the cyano groups form energetically favored trimeric hydrogen-bonding arrangements with the β-hydrogen atoms of the porphyrin cores of adjacent molecules (blue circle in

Figure 4a). Network 1 exhibits the densest structure ((0.36 ± 0.05) molecules per nm^2) of the three investigated (Figure 4).

For molecules **2** and **3**, the formation of the network is hindered by a restriction of the access of potential binding partners to the hydrogen atoms of the pyrrole units and the 4-cyanophenyl rings. As a consequence, molecules **2** and **3** do not assemble into a network at low coverage, but instead form chains through antiparallel dipole–dipole interactions. By comparing this behavior to that of molecule **1**, which readily forms trimeric structures instead of the also possible dimers even at low coverage, we conclude that without steric hindrance by an additional substituent, for the 4-cyanophenyl group, the dipole–dipole interaction is energetically less favored than the formation of trimers through hydrogen bonding. This is in agreement with a calculation by Okuno et al.[42] and was also observed for a different molecular structure with similar substituents.[54]

With increasing number of molecules **2** and **3** on the surface, the number of branches in the chains also rises (see the Supporting Information). Because the branching motifs of the chains can also be found in the networks, we assume that the growth of the network originates from the branching points once a critical ratio between the number of molecules and the free surface area is reached. In fact, STM images reveal that the transition from the chains to the networks starts with the formation of single pores (see the Supporting Information).

Similar to network 1, the alkoxy chains in network 2 (Figure 4b) are situated inside the pores and are thus separated from the cyano groups. This arrangement is possible even though the number of alkoxy chains per molecule of **2** increased by a factor of two compared with **1**. However, the corresponding higher packing density inside the pores restricts the mobility of the alkoxy chains. This results in a loss of entropy that can be compensated for by increased van der Waals interactions between the alkoxy chains.[55] The cyano groups form the energetically favored trimeric C≡N···H−C hydrogen-bonded arrangement (blue circle in Figure 4b). However, the β-hydrogen atoms of the porphyrin core cannot act as hydrogen-bond donors, presumably because the increased steric demand of the alkoxy chains prevents adjacent molecules from being as close as in the case of network 1. Therefore, the cyano group forms a hydrogen bond with the hydrogen atoms of the 4-cyanophenyl group. This results in a larger pore-to-pore distance and a decreased density of network 2 ((0.31 ± 0.02) molecules per nm^2) compared with network 1.

As described above, we assume that the formation of network 3 nucleates from chain intersections that form a single pore. However, it appears that the even higher steric demand of the larger alkoxy chains of **3** in comparison with **2** does not allow for the formation of a 4-cyanophenyl-based trimeric interaction motif, which is characteristic for network 1 and network 2. In network 3 only two molecules associate through C≡N···H−C hydrogen bonding. Tentatively, this behavior can be explained by a lack of space for a third molecule of **3** to participate in a symmetric trimeric arrangement similar to those of network 1 and network 2. Instead, a hydrogen bond is formed between the bis(alkoxy)phenyl ring of the third molecule and a cyano acceptor group of the other two molecules (cf. Figure 3b and **D** in Scheme 2). In this new asymmetric configuration, the alkoxy chains do not interfere with each other. The third molecule is then a starting point for a second pore. Due to this uncommon asymmetric assembly, half of the alkoxy chains of each molecule are found outside the pores. This leads to an even stronger restriction of their mobility, presumably amplified by an increased interaction with the substrate, and a concomitant loss of entropy, which becomes evident in the STM images by the absence of streaks in the corresponding parts of the network (Figure 4c, left) for those alkoxy chains situated outside the pores (Figure 4c, right, red circle and orange rectangle). As in network 1 and network 2, in network 3 the alkoxy chains show a tendency to associate by forming pores, in which they are still mobile, and additionally by condensation outside the pores, thereby increasing the amount of van der Waals interactions in the network. The density of network 3 is (0.30 ± 0.02) molecule per nm^2, which is comparable to that of network 2.

Conclusions

We have presented a systematic study on the influence of different alkoxyphenyl substituents on the resulting surface assemblies on a Cu(111) surface. By systematically varying the steric bulk, we showed how an elaborated change in the molecular architecture influences the resulting assembly on Cu(111) at different surface coverages. Variation of the alkoxy chains in size (chain length), number, and position controls the dimensionality of the resulting structure, that is, one-dimensional wires or two-dimensional porous networks, as well as the pore-to-pore distance in the observed networks without significantly affecting the pore diameter.

The porphyrin-based building blocks (**1**–**3**) presented in this study contain, in addition to the previously used 4-cyanophenyl rings, mono- (**1**) and dialkoxy-substituted (**2** and **3**) phenyl rings. These additional functional groups induce new assembly motifs: besides the well-established dimeric and trimeric supramolecular synthons involving the interaction between two or three cyanophenyl groups (**A** and **B** in Scheme 2), we observed in network 3 a new trimeric asymmetric interaction motif (**D** in Scheme 2). Here, one of two cyanophenyl groups of neighboring porphyrins forms a C≡N···H−C hydrogen bond with the polarized H−C residue *ortho* to the electron-withdrawing alkoxy groups of a third neighbor (cf. blue circle in Figure 4c). This hydrogen bond is also clearly revealed in a similar, but dimeric arrangement (**C** in Scheme 2), observed at branching points of the molecular chains formed by **2** and **3** at low coverages (Figure 3b).

The different assemblies are discussed in terms of the compensation of entropic losses, due to increased restriction of the flexibility of the alkoxy chains with increasing size, by

enthalpic interaction energies. This phenomenon is of general importance in the self-assembly of thermodynamically controlled systems, such as the folding of biomolecules in a cellular fluid.[56] It should be noted that for biomolecular self-assembly, solvation processes considerably affect the thermodynamics,[57] which is not the case for the dry, in vacuo assemblies studied herein.

Future work aims to exploit other supramolecular synthons known from supramolecular chemistry, directed towards supramolecular surface assemblies. In particular, the controlled change of the pore diameter, which might be possible by a sophisticated variation of the two different interaction groups (cyanophenyl and alkoxyphenyl) used in this study would be the next step to build more complex, addressable supramolecular structures with well-defined properties far beyond the currently established toolbox.

Experimental section

Synthesis: Three different zinc porphyrin derivatives (**1**–**3**) were synthesized by condensation of 5-(4-cyanophenyl)dipyrromethane with the corresponding alkoxybenzaldehydes and subsequent insertion of Zn^{2+} (see the Supporting Information).[58]

Testing the thermal stability of molecules 1–3 during sublimation: Large organic molecules often decompose under the conditions for ultra-high vacuum (UHV) sublimation. To verify the thermal stability of molecules **1**–**3**, sublimation tests were performed prior to the STM experiments at 10^{-5} mbar in a tailor-made sublimation apparatus, including a turbomolecular vacuum pump and a liquid tin heating bath (see the Supporting Information). In a typical experiment, the molecular compound (1 mg) was sublimed at bath temperatures between 380 and 420 °C within 10–30 min. ^{1}H NMR spectroscopic and mass spectrometric analysis of the sublimed compounds confirmed that porphyrin derivatives **1**–**3** sublime without fragmentation or decomposition.

STM experiments: All experiments were performed in a two-chamber UHV system (base pressure of 1×10^{-10} mbar). As a substrate for the molecular films, a (111)-oriented Cu single-crystal was used, which was cleaned by cycles of sputtering with Ar^+ ions and subsequent annealing at 800 K. By this procedure, flat terraces of about 100 nm in width separated by monoatomic steps are obtained. The molecular compounds were deposited by thermal evaporation from a commercial Knudsen-cell-type evaporator[59] onto the Cu substrate held at room temperature. In this study, the surface coverage is defined by the fraction of the surface area occupied by the deposited molecules. This can be directly determined from STM images due to the lack of a coexisting phase or a gas phase. All STM measurements were done at a sample temperature between 77 and 200 K. Temperatures >77 K were reached by PID controlled counter-heating of the sample.

Acknowledgements

This work was supported by the European Union through the Marie-Curie Research Training Network PRAIRIES, contract MRTN-CT-2006-035810, the Swiss National Science Foundation, and the NCCR "Nanoscale Science". We also thank the Swiss Federal Commission for Technology and Innovation, KTI, and Nanonis for the fruitful collaboration on the data acquisition system.

[1] J. V. Barth, *Annu. Rev. Phys. Chem.* **2007**, *58*, 375.
[2] http://www.itrs.net/reports.html
[3] a) G. Desiraju, *Crystal Engineering: The Design of Organic Solids*, Elsevier, New York, **1989**; b) M. W. Hosseini, *Acc. Chem. Res.* **2005**, *38*, 313.
[4] D. Bonifazi, H. Spillmann, A. Kiebele, M. de Wild, P. Seiler, F. Y. Cheng, H. J. Güntherodt, T. Jung, F. Diederich, *Angew. Chem.* **2004**, *116*, 4863; *Angew. Chem. Int. Ed.* **2004**, *43*, 4759.
[5] M. Wahl, M. Stöhr, H. Spillmann, T. A. Jung, L. H. Gade, *Chem. Commun.* **2007**, 1349.
[6] J.-M. Lehn, *Supramolecular Chemistry*, VCH, Weinheim, **1995**.
[7] a) K. Morgenstern, S. W. Hla, K. H. Rieder, *Surf. Sci.* **2003**, *523*, 141; b) J. Y. Grand, T. Kunstmann, D. Hoffmann, A. Haas, M. Dietsche, J. Seifritz, R. Möller, *Surf. Sci.* **1996**, *366*, 403.
[8] S. Stepanow, N. Lin, J. V. Barth, K. Kern, *J. Phys. Chem. B* **2006**, *110*, 23472.
[9] a) M. Stöhr, M. Wahl, C. H. Galka, T. Riehm, T. A. Jung, L. H. Gade, *Angew. Chem.* **2005**, *117*, 7560; *Angew. Chem. Int. Ed.* **2005**, *44*, 7394; b) G. E. Poirier, *Langmuir* **1999**, *15*, 1167; c) B. Xu, C. G. Tao, E. D. Williams, J. E. Reutt-Robey, *J. Am. Chem. Soc.* **2006**, *128*, 8493.
[10] C. B. France, P. G. Schröder, J. C. Forsythe, B. A. Parkinson, *Langmuir* **2003**, *19*, 1274.
[11] J. V. Barth, J. Weckesser, G. Trimarchi, M. Vladimirova, A. De Vita, C. Z. Cai, H. Brune, P. Günter, K. Kern, *J. Am. Chem. Soc.* **2002**, *124*, 7991.
[12] a) T. Fritz, M. Hara, W. Knoll, H. Sasabe, *Mol. Cryst. Liq. Cryst. Sci. Technol. Sect. A* **1994**, *252*, 561; b) C. Ludwig, B. Gompf, J. Petersen, R. Strohmaier, W. Eisenmenger, *Z. Phys. B* **1994**, *93*, 365; c) E. I. Altman, R. J. Colton, *Phys. Rev. B* **1993**, *48*, 18244; d) M. Kunitake, N. Batina, K. Itaya, *Langmuir* **1995**, *11*, 2337.
[13] a) M. Lackinger, S. Griessl, W. A. Heckl, M. Hietschold, G. W. Flynn, *Langmuir* **2005**, *21*, 4984; b) F. Tao, S. L. Bernasek, *Langmuir* **2007**, *23*, 3513.
[14] a) F. J. Himpsel, T. Jung, A. Kirakosian, J.-L. Lin, D. Y. Petrovykh, H. Rauscher, J. Viernow, *MRS Bull.* **1999**, *24*, 20; b) K. Aït-Mansour, P. Ruffieux, W. Xiao, P. Gröning, R. Fasel, O. Gröning, *Phys. Rev. B* **2006**, *74*, 195418.
[15] K. Tahara, S. Furukawa, H. Uji-I, T. Uchino, T. Ichikawa, J. Zhang, W. Mamdouh, M. Sonoda, F. C. De Schryver, S. De Feyter, Y. Tobe, *J. Am. Chem. Soc.* **2006**, *128*, 16613.
[16] a) M. Ruiz-Osés, N. Gonzalez-Lakunza, I. Silanes, A. Gourdon, A. Arnau, J. E. Ortega, *J. Phys. Chem. B* **2006**, *110*, 25573; b) M. E. Cañas-Ventura, W. Xiao, D. Wasserfallen, K. Müllen, H. Brune, J. V. Barth, R. Fasel, *Angew. Chem.* **2007**, *119*, 1846; *Angew. Chem. Int. Ed.* **2007**, *46*, 1814; c) J. A. Theobald, N. S. Oxtoby, M. A. Phillips, N. R. Champness, P. H. Beton, *Nature* **2003**, *424*, 1029.
[17] H. Spillmann, A. Kiebele, M. Stöhr, T. A. Jung, D. Bonifazi, F. Y. Cheng, F. Diederich, *Adv. Mater.* **2006**, *18*, 275.
[18] a) S. Stepanow, M. Lingenfelder, A. Dmitriev, H. Spillmann, E. Delvigne, N. Lin, X. B. Deng, C. Z. Cai, J. V. Barth, K. Kern, *Nat. Mater.* **2004**, *3*, 229; b) A. Dmitriev, H. Spillmann, N. Lin, J. V. Barth, K. Kern, *Angew. Chem.* **2003**, *115*, 2774; *Angew. Chem. Int. Ed.* **2003**, *42*, 2670.
[19] a) S. Buchholz, J. P. Rabe, *J. Vac. Sci. Technol. B* **1991**, *9*, 1126; b) S. De Feyter, F. De Schryver, *Top. Curr. Chem.* **2005**, *258*, 205.
[20] A. Kiebele, D. Bonifazi, F. Y. Cheng, M. Stöhr, F. Diederich, T. Jung, H. Spillmann, *ChemPhysChem* **2006**, *7*, 1462.
[21] M. Stöhr, M. Wahl, H. Spillmann, L. H. Gade, T. A. Jung, *Small* **2007**, *3*, 1336.
[22] N. Wintjes, D. Bonifazi, F. Cheng, A. Kiebele, M. Stöhr, T. Jung, H. Spillmann, F. Diederich, *Angew. Chem.* **2007**, *119*, 4167; *Angew. Chem. Int. Ed.* **2007**, *46*, 4089.
[23] S. Stepanow, N. Lin, D. Payer, U. Schlickum, F. Klappenberger, G. Zoppellaro, M. Ruben, H. Brune, J. V. Barth, K. Kern, *Angew. Chem.* **2007**, *119*, 724; *Angew. Chem. Int. Ed.* **2007**, *46*, 710.
[24] a) T. A. Jung, R. R. Schlittler, J. K. Gimzewski, H. Tang, C. Joachim, *Science* **1996**, *271*, 181; b) F. Moresco, G. Meyer, K. H. Rieder, H. Tang, A. Gourdon, C. Joachim, *Appl. Phys. Lett.* **2001**, *78*, 306; c) C. Loppacher, M. Guggisberg, O. Pfeiffer, E. Meyer, M. Bammerlin, R.

Lüthi, R. Schlittler, J. K. Gimzewski, H. Tang, C. Joachim, *Phys. Rev. Lett.* **2003**, *90*, 066107; d) F. Moresco, G. Meyer, K. H. Rieder, H. Ping, H. Tang, C. Joachim, *Surf. Sci.* **2002**, *499*, 94.
[25] T. A. Jung, R. R. Schlittler, J. K. Gimzewski, *Nature* **1997**, *386*, 696.
[26] a) S. Lee, A. B. Mallik, D. C. Fredrickson, *Cryst. Growth Des.* **2004**, *4*, 279; b) R. Paulini, K. Müller, F. Diederich, *Angew. Chem.* **2005**, *117*, 1820; *Angew. Chem. Int. Ed.* **2005**, *44*, 1788.
[27] a) G. R. Desiraju, *Angew. Chem.* **1995**, *107*, 2541; *Angew. Chem. Int. Ed. Engl.* **1995**, *34*, 2311; b) V. R. Thalladi, B. S. Goud, V. J. Hoy, F. H. Allen, J. A. K. Howard, G. R. Desiraju, *Chem. Commun.* **1996**, 401.
[28] For the application of the concept of supramolecular synthons to self-assemblies on surfaces, see: L. Scudiero, K. W. Hipps, D. E. Barlow, *J. Phys. Chem. B* **2003**, *107*, 2903.
[29] a) M. S. K. Dhurjati, J. Sarma, G. R. Desiraju, *J. Chem. Soc. Chem. Commun.* **1991**, 1702; b) D. S. Reddy, B. S. Goud, K. Panneerselvam, G. R. Desiraju, *J. Chem. Soc. Chem. Commun.* **1993**, 663; c) P. M. Ivanov, *J. Mol. Struct.* **1998**, *440*, 121.
[30] T. Yokoyama, S. Yokoyama, T. Kamikado, Y. Okuno, S. Mashiko, *Nature* **2001**, *413*, 619.
[31] a) D. Vollhardt, *J. Phys. Chem. C* **2007**, *111*, 6805; b) F. Charra, J. Cousty, *Phys. Rev. Lett.* **1998**, *80*, 1682.
[32] M. I. Boamfa, M. W. Kim, J. C. Maan, T. Rasing, *Nature* **2003**, *421*, 149.
[33] S. Weigelt, C. Busse, L. Petersen, E. Rauls, B. Hammer, K. V. Gothelf, F. Besenbacher, T. R. Linderoth, *Nat. Mater.* **2006**, *5*, 112.
[34] T. Yokoyama, S. Yokoyama, T. Kamikado, S. Mashiko, *J. Chem. Phys.* **2001**, *115*, 3814.
[35] M. Schmid, H. Stadler, P. Varga, *Phys. Rev. Lett.* **1993**, *70*, 1441; L. Bartels, G. Meyer, K. H. Rieder, *Surf. Sci.* **1999**, *432*, L621.
[36] We show an image of the network formed by porphyrin **2** here because we feel it best demonstrates the described fuzziness. Nevertheless, the effect can be observed for all three compounds investigated.
[37] a) M. Wahl, M. von Arx, T. A. Jung, A. Baiker, *J. Phys. Chem. B* **2006**, *110*, 21777; b) S. de Feyter, A. Gesquière, P. C. M. Grim, F. C. de Schryver, *Langmuir* **1999**, *15*, 2817.
[38] T. Belser, M. Stöhr, A. Pfaltz, *J. Am. Chem. Soc.* **2005**, *127*, 8720.
[39] a) M. T. Cuberes, R. R. Schlittler, J. K. Gimzewski, *Appl. Phys. A* **1998**, *66*, S669; b) T. Kamikado, T. Sekiguchi, S. Yokoyama, Y. Wakayama, S. Mashiko, *Thin Solid Films* **2006**, *499*, 329.
[40] S. Berner, M. Brunner, L. Ramoino, H. Suzuki, H. J. Güntherodt, T. A. Jung, *Chem. Phys. Lett.* **2001**, *348*, 175.
[41] The model is derived from Spartan calculations (Spartan'06, Wavefunction, Irvine, CA (USA)). Approximate arrangements of the two interacting porphyrins were taken from the surface data and simulated in the gas phase by using both PM3 and AM1 methods.
[42] Y. Okuno, T. Yokoyama, S. Yokoyama, T. Kamikado, S. Mashiko, *J. Am. Chem. Soc.* **2002**, *124*, 7218.
[43] M. Itoh, M. Takamatsu, N. Kizu, Y. Fujiwara, *J. Phys. Chem.* **1991**, *95*, 9682.
[44] T. Michinobu, C. Boudon, J.-P. Gisselbrecht, P. Seiler, B. Frank, N. N. P. Moonen, M. Gross, F. Diederich, *Chem. Eur. J.* **2006**, *12*, 1889.
[45] F. Tao, S. L. Bernasek, *J. Am. Chem. Soc.* **2005**, *127*, 12750.
[46] M. J. Crossley, L. D. Field, A. J. Forster, M. M. Harding, S. Sternhell, *J. Am. Chem. Soc.* **1987**, *109*, 341.
[47] M. Böhringer, W. D. Schneider, R. Berndt, *Angew. Chem.* **2000**, *112*, 821; *Angew. Chem. Int. Ed.* **2000**, *39*, 792.
[48] For secondary electrostatic interactions in hydrogen-bonding arrays, see: T. J. Murray, S. C. Zimmerman, *J. Am. Chem. Soc.* **1992**, *114*, 4010.
[49] Y. Köysal, S. Isýk, N. Akdemir, E. Agar, C. Kantar, *Acta Crystallogr. E* **2004**, *60*, O930.
[50] a) D. Britton, *J. Chem. Crystallogr.* **1991**, *2127*, 405; b) U. Drück, A. Kutoglu, *Acta Crystallogr. C* **1983**, *39*, 638.
[51] S. De Feyter, F. C. De Schryver, *Chem. Soc. Rev.* **2003**, *32*, 139.
[52] G. M. Whitesides, J. P. Mathias, C. T. Seto, *Science* **1991**, *254*, 1312.
[53] L. Wang, D. Qi, L. Liu, S. Chen, X. Gao, A. T. S. Wee, *J. Phys. Chem. C* **2007**, *111*, 3454.
[54] L. Gross, K. H. Rieder, A. Gourdon, C. Joachim, F. Moresco, *ChemPhysChem* **2007**, *8*, 245.
[55] L. Merz, H. J. Güntherodt, L. J. Scherer, E. C. Constable, C. E. Housecroft, M. Neuburger, B. A. Hermann, *Chem. Eur. J.* **2005**, *11*, 2307.
[56] K. K. Frederick, M. S. Marlow, K. G. Valentine, A. J. Wand, *Nature* **2007**, *448*, 325; R. S. Spolar, M. T. Record, *Science* **1994**, *263*, 777.
[57] J. M. Sturtevant, *Proc. Natl. Acad. Sci. USA* **1977**, *74*, 2236.
[58] a) C. H. Lee, J. S. Lindsey, *Tetrahedron* **1994**, *50*, 11427; b) B. J. Littler, Y. Ciringh, J. S. Lindsey, *J. Org. Chem.* **1999**, *64*, 2864; c) L. H. Yu, J. S. Lindsey, *J. Org. Chem.* **2001**, *66*, 7402.
[59] See www.kentax.de.

Received: April 18, 2008
Published online: May 30, 2008

